# Nonuniformity Characterization of CdTe Solar Cells Using LBIC

Russell M. Geisthardt and James R. Sites

***Abstract*—Light-beam-induced current measurements have been used for characterization of nonuniformities in cadmium telluride (CdTe) solar cells. Spectral dependence, voltage-bias dependence, and resolution dependence are used for detailed characterization of nonuniformities in junction quality, window thickness, and absorber band gap. These tools were applied to CdTe cells and used to identify thin regions in the CdS layer, regions of modified band gap, and weak diode regions. In addition, an improved procedure has allowed for shorter measurement times without discernable loss of accuracy.**

***Index Terms*—Cadmium telluride (CdTe), characterization, light-beam-induced current (LBIC), nonuniformity, photovoltaic (PV) cells.**

## I. Introduction

ONE significant problem facing cadmium telluride (CdTe) solar cells is nonuniformity. For nonuniformities that affect the short-circuit current, local quantum efficiency (QE) measurements using light-beam-induced current (LBIC) measurements have been used for many years [1]–[3].

A common problem with LBIC, which has limited its industrial applicability, is the long measurement time. This is a combination of motion time and measurement time. A procedure has been developed and is described in this study for on-the-fly measurement, which reduced the required time by a factor of 3–9 with little or no loss of position or measurement accuracy.

Reduction in measurement time makes it easier to take many scans of a single cell using variations in wavelength and applied voltage bias. This study presents a general strategy to use LBIC tools for nonuniformity characterization of CdTe cells. An additional 405-nm wavelength has been added to existing longer wavelengths to identify problems related to the solar-cell window layer. The effects on nonuniformities under different wavelengths, applied biases, and resolutions are explored, using both area maps and line scans.

## II. Experimental Details

The LBIC configuration used in this study is depicted in Fig. 1 and was described in [3]–[5]. Light is provided by a laser diode and directed through a fiber. A computer-controlled attenuator is used to control light intensity to keep the spot at the sample on the order of 100 mW/cm$^2$. The light is collimated and polarized. A portion of the beam is split off for intensity monitoring. The remaining beam is chopped with an optical chopper and directed onto the cell. A microscope objective is used for focusing. Stepper motors are used to control the focusing, as well as to raster the cell under the laser for scanning. Output from the cell is sent to a preamplifier and measured using a lock-in amplifier. The preamplifier can also be used to apply a voltage bias to the cell. The entire system is controlled using a computer with home-built LabView software. Light bias had little impact on QE of these CdTe cells and has generally been avoided because it degrades the signal-to-noise ratio. QE values are calculated as the ratio of cell current to photon current. The photon current is determined by using a reference device of known QE. The values are generally consistent with the QE values measured using a large-area QE system.

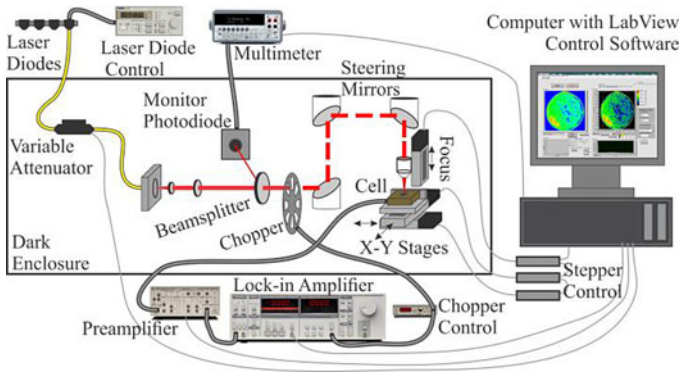


Fig. 1. Diagram of the LBIC setup.

The laser spot sizes used in this study are 100, 10, or 1 $\mu$m. Areas are mapped with 100 points $\times$ 100 points, with the step size half the spot size, which gives an overlap between adjacent points. Standard measurement areas for these spot sizes, therefore, are 5000 $\mu$m $\times$ 5000 $\mu$m, 500 $\mu$m $\times$ 500 $\mu$m, and 50 $\mu$m $\times$ 50 $\mu$m, respectively.

Several updates have been made to the original system to improve the functionality. A 405-nm laser was added, in addition to existing 638-, 830-, and 850-nm lasers. The 405-nm laser allows exploration of the wide-band-gap window layers used in most thin-film cells. The system previously used electronic modulation of the laser current to achieve ac light; however, this was found to be less stable and more noisy than the optical chopper (SRS SR540) now used. The previous monitor system using a home-built preamplifier and lock-in has been replaced

Manuscript received November 25, 2013; revised March 11, 2014; accepted March 26, 2014. Date of publication April 14, 2014; date of current version June 18, 2014. This work was supported by the U.S. Department of Energy F-PACE under Award DE-EE0005399 and by the National Science Foundation under I/UCRC for Next Generation Photovoltaics.

The authors are with the Department of Physics, Colorado State University, Fort Collins, CO 80523 USA (e-mail: russell.geisthardt@gmail.com; sites@lamar.colostate.edu).

Digital Object Identifier 10.1109/JPHOTOV.2014.2314575

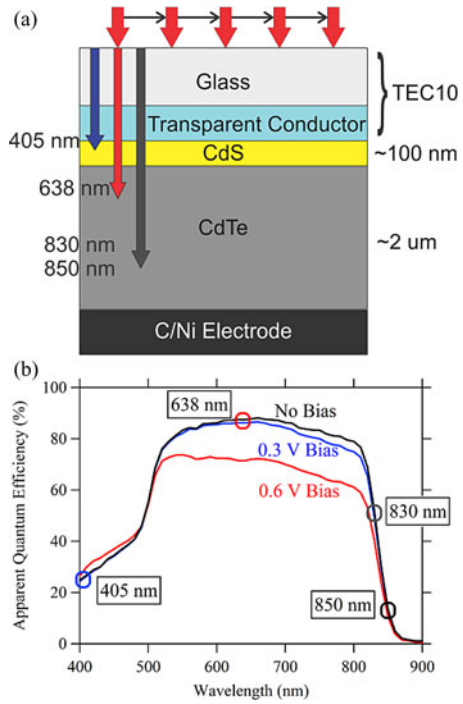


Fig. 2. (a) Schematic of the cell. Arrows on the left illustrate approximate average absorption areas of the different laser wavelengths. (b) QE of one of the cells used at varying voltage biases. The wavelengths used in LBIC scans are circled.

by an amplified photodiode (Thorlabs PDA100A) read by a digital multimeter (Chroma 12061).

The CdTe cells for this study were fabricated in the CSU PV Manufacturing Lab. A schematic is shown in Fig. 2(a). CdS and CdTe were deposited on TEC10 glass by closed-space sublimation. $CdCl_2$ was sublimated, annealed, and removed before copper was added. The devices were finished with a carbon/nickel paint and delineated into circular devices of about 1-cm diameter. Unless otherwise noted, the cell had an efficiency of 13%. Further descriptions of device fabrication can be found in [6] and [7].

Fig. 2(b) shows the QE response of one of the cells used. The wavelengths used in the following sections for LBIC are circled. Voltage biases are also applied, so response at varying bias is included. Fig. 2(a) shows generally where the different laser wavelengths are absorbed in the cell. The absorption will fall off exponentially with distance; therefore, these arrows illustrate an approximate average depth of absorption.

## III. Reduced Light-Beam-Induced Current Measurement Time

### A. Replacing Stepped Process With Continuous Process

The previous LBIC measurement technique used a discrete measurement process to record an image of 10 000 points. The system commanded the cell to the desired position, paused until it arrived, then took a measurement, and moved to the next position. This resulted in wait times as long as 200 ms between points, in addition to a measurement time of approximately

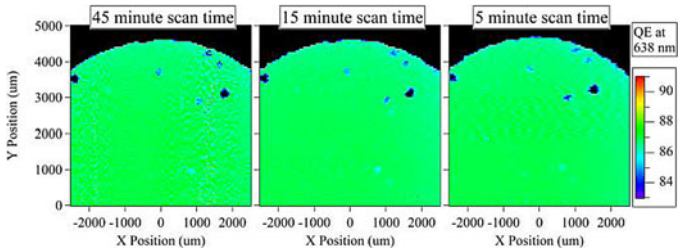


Fig. 3. Comparison of point-by-point (left), fixed-time (center), and free-time (right) LBIC scans. There is a minor distortion with the fastest scan, but no other significant differences. Scans are at 638 nm with no applied bias and 100-$\mu$m spot size. Cell efficiency is 13%.

55 ms. The result was a scan time over a standard 10 000-point measurement area of 45 min.

To reduce the measurement time, a procedure was developed with continuous motion. This on-the-fly technique commands the system to move all the way across the scan area and measures continuously as the cell moves. There is some delay in the software processing which can introduce slight fluctuations in the time between data points. Because of this fluctuation, a feature was built in, which allows the user to choose either a constant measurement cycle time (which introduces a slight delay and increases the total scan time) or the free measurement time. The free measurement time choice reduces the total scan time, but the data points are not necessarily equally spaced. With a constant measurement time, the total scan takes 15 min, and with the free measurement time, the time is 5 min. Thus, the total scan time has been reduced by a factor of 3 or 9, respectively. Fig. 3 shows comparisons of nearly identical scan results using the three different approaches. There are some additional features on the right side of the 45-min scan, which are caused by laser noise and are generally discounted.

There are, however, potential pitfalls with this procedure. Since the steppers do not stop for each data point, there is a potential for blurring between adjacent points. This concern is reduced by the fact that there is already an overlap of the points. It can be further reduced by increasing the chopping frequency or reducing the lock-in time constant. The well-defined features in Fig. 3 show that there is no discernable problem. An additional potential problem is a position offset or inconsistent spacing of points. Again, this problem is not apparent in Fig. 3. Further, this problem can be addressed by using the fixed measurement time or by using recorded positions when graphing data. The fixed-time procedure was used for the all following scans.

### B. Line Scan and Area Selector Tools

An additional tool was developed to save user time by speeding up selection of areas for higher resolution scans or for line scans. This tool allows a user to display a data map, select a smaller area, and immediately measure that area with higher resolution. This avoids accidentally missing interesting features or needing to use an extra program to graph data first. A line scan feature was also added, which provides quantitative data with no additional measurement time required.

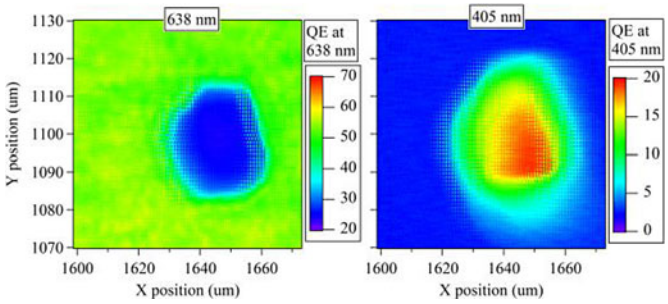


Fig. 4. Thin spot in CdS characterized by reduce response at 638 nm (left) and increased response at 405 nm (right). Scans are with no applied bias and 1-$\mu$m spot size. The cell has a relatively low 8.5% efficiency.

## IV. Nonuniformity Characterization

To fully characterize solar-cell nonuniformities and identify their sources, a single scan is often insufficient, and additional measurement parameters are needed. In this study, the spectral and voltage-bias dependence of the nonuniformities is characterized, and nonuniformities are scanned at different resolutions.

### A. Spectral Dependence

The addition of the 405-nm wavelength laser has made characterization of the window layer, generally CdS, possible. One common concern with thin CdS is nonuniform deposition, including pinholes, which can degrade performance through weak diode regions [8], [9]. Since absorption in the CdS does not contribute significantly to $J_{sc}$, cell response at short wavelengths depends on the thickness of the CdS. Thinner CdS allows more light to pass to the CdTe where it can be absorbed and collected. Thus, increased response at 405 nm shows thinner CdS. Fig. 4 shows an example of a thin spot, approximately 20 $\mu$m in diameter, in the CdS layer. It is characterized by an increased response at 405 nm because of higher transmission through the CdS, and lower response at 638 nm because of reduced junction quality. The data suggest that this is not a pinhole, because a true hole through the CdS should eliminate any absorption losses at 405 nm. In this case, however, the QE of the cell only increases to 20%, which suggests a reduction in CdS thickness, but not a complete hole.

Other nonuniformities can be characterized by using all four wavelengths. Fig. 5 shows LBIC scans at four wavelengths. Because of low laser power, the 405- and 830-nm scans have higher noise. Some features are apparent at some wavelengths, but not others. The feature covered by the line in the upper right of the 638-nm scan is explored by line scans in Fig. 6. The line scan shows that the feature causes reduced response at 638 and 830 nm, no real change at 405 nm, and increased response at 850 nm. Since 850 nm is very near the band edge of the CdTe, the increased response at 850 nm is due to a shift to a lower band gap, which is usually attributed to sulfur diffusion into the CdTe [10]. A high-sulfur area might also cause electrical issues which reduce the signal. This reduction overwhelms any increase in signal at 830 nm due to a shift in the band gap. Note that the fine structure at 638 nm appears also in the 830-nm signal.

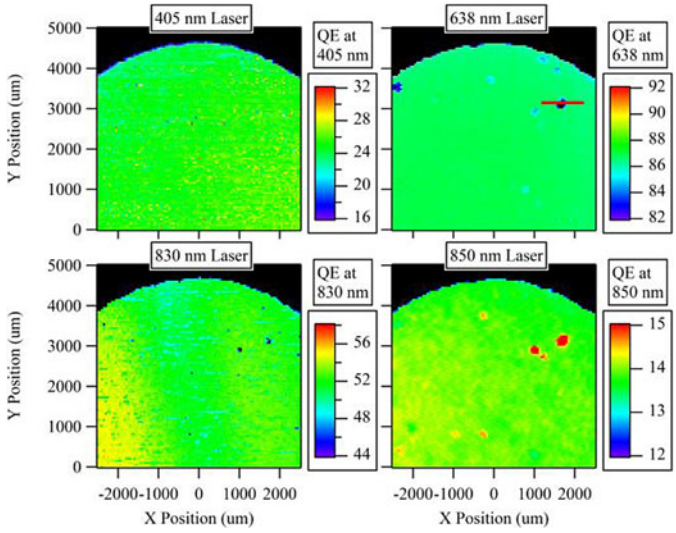


Fig. 5. LBIC scans at four wavelengths. The line in the upper right is shown as a line scan in Fig. 6. Scans are with no applied bias and 100-$\mu$m spot size.

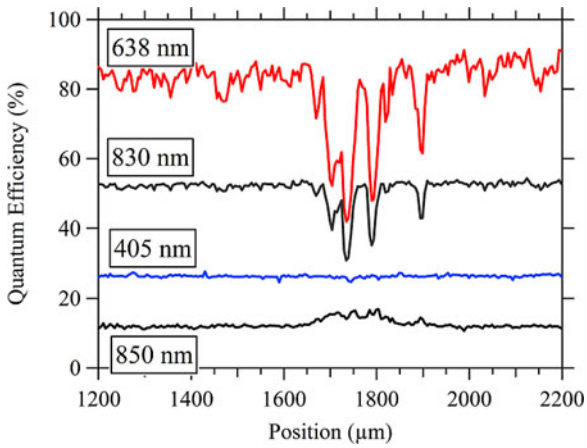


Fig. 6. Line scans of a feature which varies in response with wavelength. Scans are with no applied bias and 10-$\mu$m spot size.

### B. Voltage-Bias Dependence

The measured, or apparent, QE of an entire cell is expected to decrease as a forward bias is applied, as seen in Fig. 3. However, the response to applied bias is often nonuniform over the cell. Regions of weak diodes (high $J_0$) will have their QE reduced faster than regions with stronger diodes (lower $J_0$) [11]. Fig. 7 shows how the nonuniformity in the cell increases with increasing voltage bias, with new features appearing in far forward bias. The line in the upper left of the zero-voltage-bias scan is shown as a line scan in Fig. 8. This figure shows a weak diode feature that has a small area of influence (<50 $\mu$m) and small impact on QE (<5%) at no applied bias. At large forward bias, the feature grows to nearly 200 $\mu$m and a 30% drop in QE. The apparent QE even becomes negative at 0.8 V forward bias and above. This is consistent with a weak diode that has passed the $V_{oc}$ point, where light–dark crossover in CdTe cells commonly appears. Note that in Fig. 8 also, the fine structure is consistent among the scans, implying that the small variations in response are real.

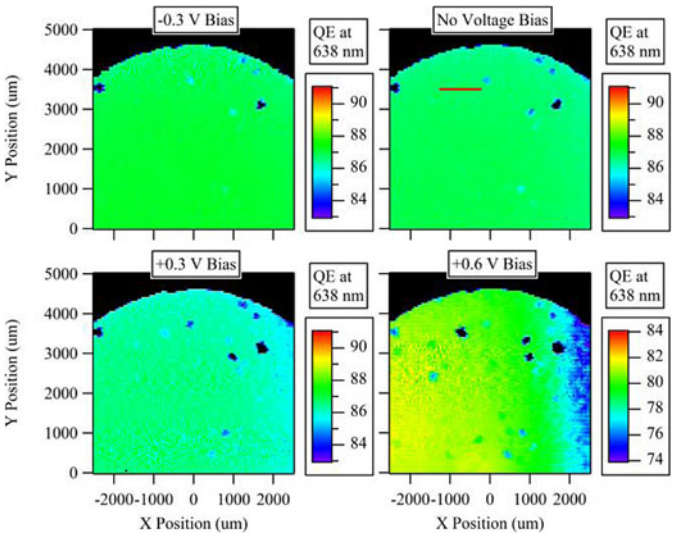


Fig. 7. LBIC scans at four voltage biases. The line in the upper right is shown as a line scan in Fig. 8. Scans are at 638 nm and 100-$\mu$m spot size.

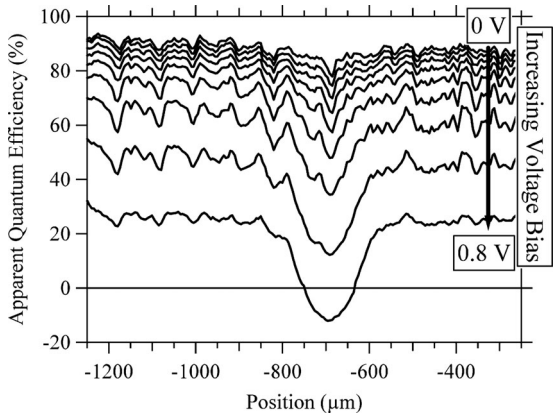


Fig. 8. Line scan of a feature which changes in response with applied bias. Scans are at 638 nm and 10-$\mu$m spot size.

### C. Resolution Dependence

Since nonuniformities exist on many different scales, it is useful to be able to change the scan resolution. Three standard resolutions in our system are 100-, 10-, and 1-$\mu$m spot sizes. Diffraction limits the spot size to around 1 $\mu$m; therefore, features smaller than this cannot be resolved using traditional optical methods. The process of measuring features at higher resolutions is assisted by the area selector tool described in Section III-B. Fig. 9 shows area scans at three increasing resolutions. The defect covered by the line scan in Fig. 6 is shown in the medium-resolution (10-$\mu$m spot size) scan. The medium-resolution scan shows that the feature is roughly circular with a 200-$\mu$m diameter and some interior features, which agrees with the line scan. Features are visible in the high-resolution scan which vary in QE by 5% and are roughly 30 $\mu$m in size. These features do not appear in the lowest resolution scan because they are averaged by the 100-$\mu$m spot size.

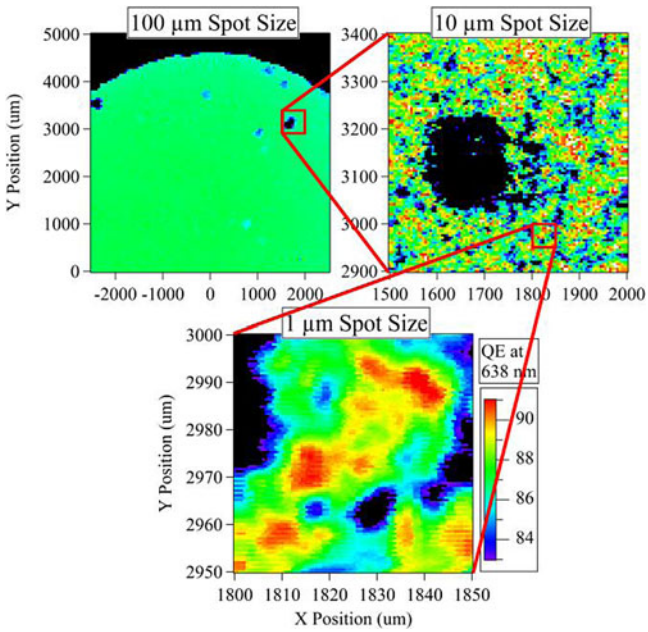


Fig. 9. Area scans at three resolutions. Scans are at 638 nm with no applied bias.

## V. Conclusion

An on-the-fly measurement procedure has reduced the scan time for an LBIC system by a factor of 9. When coupled with tools to select areas and line scans, this greatly improves the flexibility and throughput of the LBIC system.

LBIC with wavelength and voltage-bias variation is a powerful tool for characterizing defects and for aiding in identification of causes of defects. Using these tools, we have identified areas of thin CdS, likely sulfur diffusion into CdTe, and weak diodes. These tools could be used for identification of other defects in many types of cells. Additional information can be achieved by looking at additional wavelengths under voltage bias or light bias.

## Acknowledgment

The authors would like to thank K. Cameron, K. Barth, and M. Tashkandi for manufacturing the cells used in this work. They would also like to thank J. Raguse, Z. Huang, and D. Swanson for helpful conversations and suggestions in this work.

## References

[1] C. H. Seager, "The determination of grain-boundary recombination rates by scanned spot excitation methods," *J. Appl. Phys.*, vol. 53, no. 8, pp. 5968–5971, Aug. 1982.

[2] J. Marek, "Light-beam-induced current characterization of grain boundaries," *J. Appl. Phys.*, vol. 55, no. 2, pp. 318–326, Jan. 1984.

[3] J. F. Hiltner and J. R. Sites, "High resolution laser stepping measurements on polycrystalline solar cells," in *Proc. 16th Eur. Photovoltaic Sol. Energy Conf.*, Glasgow, U.K., 2000, pp. 650–653.

[4] J. F. Hiltner, "Investigation of spatial variations in collection efficiency of solar cells," Ph.D. dissertation, Dept. Phys., Colorado State Univ., Fort Collins, CO, USA, 2001.

[5] J. R. Sites and T. J. Nagle, "LBIC analysis of thin-film polycrystalline solar cells," in *Proc. 31st IEEE Photovoltaics Spec. Conf.*, 2005, pp. 199–204.

[6] P. S. Kobyakov, J. M. Kephart, and W. S. Sampath, "Sublimation of Mg onto CdS/CdTe films fabricated by advanced deposition system," in *Proc. 37th IEEE Photovoltaic Spec. Conf.*, Seattle, WA, USA, 2011, pp. 002740–002745.
[7] D. E. Swanson, R. M. Geisthardt, J. T. McGoffin, J. D. Williams, and J. R. Sites, "Improved CdTe solar cell performance by plasma cleaning the TCO layer," *IEEE J. Photovoltaics*, vol. 3, no. 2, pp. 838–842, Apr. 2013.
[8] M. Tashkandi, "Pinholes and morphology of CdS films: The effect on the open circuit voltage of CdTe solar cells," Ph.D. dissertation, Dept. Mech. Eng., Colorado State Univ., Fort Collins, CO, USA, 2012.
[9] W. S. M. Brooks, S. J. C. Irvine, and V. Barrioz, "High-resolution laser beam induced current measurements on $Cd_{0.9}Zn_{0.1}S$/CdTe solar cells," *Energy Procedia*, vol. 10, pp. 232–237, 2011.
[10] K. Ohata, J. Saraie, and T. Tanaka, "Optical energy gap of the mixed crystal $CdS_xTe_{1-x}$," *Jpn. J. Appl. Phys.*, vol. 12, no. 10, pp. 1641–1642, 1973.
[11] M. Gloeckler and J. R. Sites, "Quantum efficiency of CdTe solar cells in forward bias," in *Proc. 19th Eur. Photovoltaic Sol. Energy Conf.*, Paris, France, 2004, pp. 1863–1866.

**Russell M. Geisthardt** received the B.A. degree in physics from Lawrence University, Appleton, WI, USA, in 2008 and the M.S. degree in physics from Colorado State University, Fort Collins, CO, USA, in 2011, where he is currently working toward the Ph.D. degree.

**James R. Sites** received the B.S. degree from Duke University, Durham, NC, USA, in 1965 and the M.S. and Ph.D. degrees from Cornell University, Ithaca, NY, USA, in 1968 and 1969, respectively.

Since 1971, he has been with Colorado State University, Fort Collins, CO, USA, where he has been involved in research on device physics of thin-film, polycrystalline solar cells.